Journal of Statistical Physics (2019) 177:960–983
https://doi.org/10.1007/s10955-019-02404-2

Subcarrier Domain of Multicarrier Continuous-Variable Quantum Key Distribution

Laszlo Gyongyosi[1,2,3] · **Sandor Imre**[2]

Received: 4 May 2018 / Accepted: 3 October 2019 / Published online: 23 October 2019

Abstract
The subcarrier domain of multicarrier continuous-variable quantum key distribution (CVQKD) is defined. In a multicarrier CVQKD scheme, the information is granulated into Gaussian subcarrier CVs and the physical Gaussian link is divided into Gaussian subchannels. The subcarrier domain injects physical attributes to the description of the subcarrier transmission. We prove that the subcarrier domain is a natural representation of the subcarrier-level transmission in a multicarrier CVQKD scheme. We also extend the subcarrier domain to a multiple-access multicarrier CVQKD setting. We demonstrate the results through the adaptive multicarrier quadrature-division (AMQD) CVQKD scheme and the AMQD-MQA (multiuser quadrature allocation) multiple-access multicarrier scheme. The subcarrier domain representation provides a general apparatus that can be utilized for an arbitrary multicarrier CVQKD scenario.

Keywords Quantum key distribution · Quantum cryptography · Quantum continuous variables · CVQKD

1 Introduction

The continuous-variable quantum key distribution protocols allow for the parties to establish an unconditionally secure communication over the traditional telecommunication networks [1–20]. In comparison to discrete-variable (DV) QKD, the CVQKD schemes do not require single-photon devices, a fact that allows us to implement in practice by standard devices [21–31]. Despite the several attractive benefits of CVQKD [1–3,9–14], these protocols still require

Communicated by Alessandro Giuliani.

✉ Laszlo Gyongyosi
lasgy_ph@yahoo.com

[1] School of Electronics and Computer Science, University of Southampton, Southampton SO17 1BJ, UK

[2] Department of Networked Systems and Services, Budapest University of Technology and Economics, Budapest 1117, Hungary

[3] MTA-BME Information Systems Research Group, Hungarian Academy of Sciences, Budapest 1051, Hungary

significant performance improvements to be comparable with that of the traditional telecommunications [32–49]. For this purpose, the multicarrier CVQKD has been defined through the adaptive multicarrier quadrature division (AMQD) modulation [5]. In a multicarrier CVQKD system, the Gaussian input CVs are granulated into subcarrier Gaussian CVs via the inverse Fourier transform, which are decoded by the receiver by the unitary CVQFT (continuous-variable quantum Fourier transform) operation [5]. Precisely, the multicarrier transmission divides the physical Gaussian link into several Gaussian sub-channels, where each sub-channel is dedicated for the conveying of a Gaussian subcarrier CV. In particular, the multicarrier transmission injects several benefits to CVQKD, such as improved secret key rates, higher tolerable excess noise, and enhanced transmission distances [5,6,8,9,29–31,50–57]. Specifically, the benefits of the multicarrier CVQKD modulation has been extended to a multiple-access CVQKD through the AMQD-MQA (multiuser quadrature allocation) scheme [8], in which the simultaneous reliable transmission of the legal users is handled through the sophisticated allocation mechanism of the Gaussian subcarriers. The SVD-assisted (singular value decomposition) AMQD injects further extra degrees of freedom into the transmission [29,52], which can also be exploited in a multiple-access multicarrier CVQKD.

The achievable secret key rates in a multicarrier CVQKD setting have been rigorously derived in [6]. These secret key rates also confirm the multimode bounds determined in [43] (see the results on fundamental rate-loss scaling in quantum optical communications in [43]). For further information on the bounds of private quantum communications, we suggest [44].

Here, we provide a natural representation of the subcarrier CV transmission and show that it also allows us to utilize the physical attributes into the sub-channel modeling. The angular domain representation is a useful tool in traditional telecommunications to model the physical signal propagation through a communication channel. The angular domain representation is aimed at revealing and verifying the connections of the physical layer and the mathematical channel model in different scenarios, avoiding the use of an inaccurate channel representation [58–60]. Here, we show that similar benefits can be brought up to multicarrier CVQKD. We define the subcarrier domain representation for multicarrier CVQKD. The subcarrier domain utilizes the phase-space angles of the Gaussian subcarrier CV to construct the model of a Gaussian sub-channel and to build an appropriate statistical model of subcarrier transmission. The subcarrier domain is an adequate application for multicarrier CVQKD since it is a natural representation of the CVQFT operation. The key behind the subcarrier domain representation is the Fourier operation, which has a central role in a multicarrier CVQKD setting since this operation makes possible the construction of Gaussian subcarrier CVs from the single-carriers and Gaussian sub-channels from the physical Gaussian link.

Particularly, the CVQFT transformation not just opens the door for the characterization of the subcarrier domain of a Gaussian sub-channel but also provides us a framework to study the effects of psychical layer transmission in an experimental multicarrier CVQKD scenario. The subcarrier domain utilizes physical attributes such as the phase space angle into the description of the transmission. Thus, the subcarrier domain representation takes into account not just the theoretical model but also the physical level of the subcarrier transmission. Since the subcarrier domain is a natural representation of a multicarrier CVQKD transmission, it allows us to extend it to a multiple-access multicarrier CVQKD setting. Furthermore, the subcarrier domain model provides a general framework for any experiential multicarrier CVQKD.

The novel contributions of our manuscript are as follows:

1. *We define the subcarrier domain of multicarrier continuous-variable quantum key distribution.*

2. *The subcarrier domain injects physical attributes to the description of the subcarrier transmission.*
3. *We prove that the subcarrier domain is a natural representation of the subcarrier-level transmission in a multicarrier CVQKD scheme.*
4. *We extend the subcarrier domain to a multiple-access multicarrier CVQKD setting. We demonstrate the results through the adaptive multicarrier quadrature-division (AMQD) CVQKD scheme and the AMQD-MQA (multiuser quadrature allocation) multiple-access multicarrier scheme.*
5. *The subcarrier domain representation provides a general apparatus that can be utilized for an arbitrary multicarrier CVQKD scenario. The framework is particularly convenient for experimental multicarrier CVQKD scenarios.*

This paper is organized as follows. In Sect. 2, some preliminaries are briefly summarized. Section 3 discusses the subcarrier domain representation for multicarrier CVQKD. Section 4 extends the subcarrier domain for multiple-access multiuser CVQKD. Finally, Sect. 5 concludes the results. Supplemental information is included in the Appendix.

2 Preliminaries

The basic terms and notations of multicarrier CVQKD are summarized in Sect. A.1 of the Appendix. The detailed description of AMQD and AMQD-MQA can be found in [5] and [8]. For the secret key rate formulas, see [6].

3 Subcarrier Domain of Multicarrier CVQKD

Proposition 1 (Subcarrier domain representation of multicarrier transmission.) *For the i-th Gaussian sub-channel $\mathcal{N}_i$, the subcarrier domain representation is $\mathcal{R}_{\phi_i}\left(T_i\left(\mathcal{N}_i\right)\right) = UT_i\left(\mathcal{N}_i\right)U$, where U is the CVQFT operator.*

Proof The proofs throughout assume l Gaussian sub-channels for the multicarrier transmission. The angles of the $|\phi_i\rangle$ transmitted and the $\left|\phi_i'\right\rangle$ received subcarrier CVs in the phase space $\mathcal{S}$ are denoted by $\theta_i^* \in [0, 2\pi]$, and $\theta_i \in [0, 2\pi]$, respectively.

Specifically, first, we express $F\left(\mathbf{T}\left(\mathcal{N}\right)\right)$ as

$$\begin{aligned} F\left(\mathbf{T}\left(\mathcal{N}\right)\right) &= \sum_{l} F\left(T_i\left(\mathcal{N}_i\right)\right) \\ &= \sum_{i=0}^{l-1}\sum_{k=0}^{l-1} T_k e^{\frac{-i2\pi ik}{l}}, \end{aligned} \tag{1}$$

from which $F\left(T_i\left(\mathcal{N}_i\right)\right)$ is yielded as

$$F\left(T_i\left(\mathcal{N}_i\right)\right) = \sum_{k=0}^{l-1} T_k e^{\frac{-\mathrm{i}2\pi ik}{l}}. \tag{2}$$

Next, we recall the attributes of a multicarrier CVQKD transmission from [5]. In particular, assuming l Gaussian sub-channels, the output $\mathbf{y}$ is precisely as follows:

$$\begin{aligned}\mathbf{y} &= F\left(\mathbf{T}\left(\mathcal{N}\right)\right) F\left(\mathbf{d}\right) + F\left(\Delta\right) \\ &= F\left(\mathbf{T}\left(\mathcal{N}\right)\right) F\left(F^{-1}\left(\mathbf{z}\right)\right) + F\left(\Delta\right) \\ &= \left(F\left(\mathbf{T}\left(\mathcal{N}\right)\right) F\right)\mathbf{d} + F\left(\Delta\right) \\ &= \sum_{l} F\left(T_i\left(\mathcal{N}_i\right)\right) d_i + F\left(\Delta_i\right),\end{aligned} \tag{3}$$

where

$$F\left(\mathbf{d}\right) = F\left(F^{-1}\left(\mathbf{z}\right)\right) = \mathbf{z}. \tag{4}$$

The l columns of the $l \times l$ unitary matrix F formulate basis vectors, which are referred to as the domain $\mathcal{R}_{\phi_i}$, from which the subcarrier domain representation $\mathcal{R}_{\phi_i}\left(T_i\left(\mathcal{N}_i\right)\right)$ of $T_i\left(\mathcal{N}_i\right)$ is defined as

$$\mathcal{R}_{\phi_i}\left(T_i\left(\mathcal{N}_i\right)\right) = F\left(T_i\left(\mathcal{N}_i\right)\right) F. \tag{5}$$

Thus, (3) can be rewritten as

$$\begin{aligned}\mathbf{y}^{\mathcal{R}_\phi} &= \mathcal{R}_\phi\left(\mathbf{T}\left(\mathcal{N}\right)\right)\mathbf{d} + F\left(\Delta\right) \\ &= \sum_{l} \mathcal{R}_{\phi_i}\left(T_i\left(\mathcal{N}_i\right)\right) d_i + F\left(\Delta_i\right),\end{aligned} \tag{6}$$

where $\mathbf{y}^{\mathcal{R}_\phi}$ is referred to as the subcarrier domain representation of $\mathbf{y}$.

Particularly, from (5) follows that $\mathcal{R}_{\phi_i}\left(T_i\left(\mathcal{N}_i\right)\right)$ can be expressed as

$$\mathcal{R}_{\phi_i}\left(T_i\left(\mathcal{N}_i\right)\right) = U T_i\left(\mathcal{N}_i\right) U, \tag{7}$$

where U is an $l \times l$ unitary matrix as

$$U = F, \tag{8}$$

where F refers to the CVQFT operator which for l subcarriers can be expressed by an $l \times l$ matrix, as

$$U = \frac{1}{\sqrt{l}} e^{\frac{-\mathrm{i}2\pi ik}{l}}, i, k = 0, \ldots, l-1, \tag{9}$$

thus,

$$\mathcal{R}_{\phi_i}\left(\mathbf{T}\left(\mathcal{N}\right)\right) = \sum_{i=1}^{l} U\left(T_i\left(\mathcal{N}_i\right)\right). \tag{10}$$

To conclude, the results in (1) and (2) can be rewritten as

$$U\left(\mathbf{T}\left(\mathcal{N}\right)\right) = \sum_{i=1}^{l} U\left(T_i\left(\mathcal{N}_i\right)\right), \tag{11}$$

thus

$$F\left(T_i\left(\mathcal{N}_i\right)\right) = U\left(T_i\left(\mathcal{N}_i\right)\right). \tag{12}$$

Specifically, an arbitrary distributed $\mathcal{R}_{\phi}\left(\mathbf{T}\left(\mathcal{N}\right)\right)$ can be approximated via an averaging over the following statistics:

$$\mathcal{S}\left(\mathcal{R}_{\phi}\left(\mathbf{T}\left(\mathcal{N}\right)\right)\right) \in \mathcal{CN}\left(0, \sigma^2_{\mathbf{T}(\mathcal{N})}\right), \tag{13}$$

by theory.

Since the unitary U operation does not change the distribution of $\mathcal{S}\left(\mathbf{T}\left(\mathcal{N}\right)\right)$, an arbitrarily distributed $\mathbf{T}\left(\mathcal{N}\right)$ can be approximated via an averaging over the statistics of

$$\mathcal{S}\left(\mathbf{T}\left(\mathcal{N}\right)\right) \in \mathcal{CN}\left(0, \sigma^2_{\mathbf{T}(\mathcal{N})}\right). \tag{14}$$

□

Theorem 1 *(Subcarrier domain of a Gaussian sub-channel). The $\mathcal{R}_{\phi_i}$ subcarrier domain representation of $\mathcal{N}_i, i = 0 \ldots l-1$, is $\mathcal{R}_{\phi_i}\left(T_i\left(\mathcal{N}_i\right)\right) = \sum_k \mathrm{A}\left(\mathcal{N}_i\right) b\left(k/l\right)^{\dagger} b\left(\cos\theta_i\right) b\left(\cos\theta_i^*\right)^{\dagger} b\left(i/l\right)$, $k = 0 \ldots l-1$, where $b\left(\cdot\right)$ is an orthonormal basis vector of $\mathcal{R}_{\phi_i}$, θ_i^* and θ_i are the phase-space angles of $|\phi_i\rangle$ and $\left|\phi_i'\right\rangle$, $\mathrm{A}\left(\mathcal{N}_i\right) = x_i$, where x_i is a real variable, $x_i \geq 0$.*

Proof The b basis vectors of $\mathcal{R}_{\phi_i}$ are evaluated as follows. Let $\theta_i^* \in [0, 2\pi]$ refer to the angle of the i-th noise-free input Gaussian subcarrier CV $|\phi_i\rangle$ in $\mathcal{S}$. The angle of the i-th noisy subcarrier CV $\left|\phi_i'\right\rangle$ is referred to as $\theta_i \in [0, 2\pi]$, $\theta_i \neq \theta_i^*$.

In particular, for the subcarrier domain representation, the scaled CVQFT operation defines the $b\left(\cdot\right)$ basis at l Gaussian sub-channels as an $l \times 1$ matrix:

$$b\left(\cos\theta_i\right) = \frac{1}{\sqrt{l}} \begin{pmatrix} 1 \\ e^{-i2\pi\cos\theta_i} \\ e^{-i2\pi 2\cos\theta_i} \\ \vdots \\ e^{-i2\pi(l-1)\cos\theta_i} \end{pmatrix}, \tag{15}$$

while for the input angle θ_i^* also defines an $l \times 1$ matrix as

$$b\left(\cos\theta_i^*\right) = \frac{1}{\sqrt{l}} \begin{pmatrix} 1 \\ e^{-i2\pi\cos\theta_i^*} \\ e^{-i2\pi 2\cos\theta_i^*} \\ \vdots \\ e^{-i2\pi(l-1)\cos\theta_i^*} \end{pmatrix}. \tag{16}$$

Precisely, the difference of the cos functions of the i-th θ_i^* transmitted and the θ_i received angles is defined as

$$\tau_i = \cos\theta_i - \cos\theta_i^*. \tag{17}$$

Let $b\left(\cos\theta_i\right)$ and $b\left(\cos\theta_i^*\right)$ be the basis vectors of $\cos\theta_i$, $\cos\theta_i^*$ [58–60], then for the $\Omega_i = \theta_i - \theta_i^*$ angle

$$\left|\cos\Omega_i\right| = \left|b\left(\cos\theta_i^*\right)^{\dagger} b\left(\cos\theta_i\right)\right|, \tag{18}$$

and

$$\left|\cos\Omega_i\right| = \left|f\left(\tau_i\right)\right|, \tag{19}$$

where [58]

$$f\left(\tau_i\right) = \frac{1}{l} e^{\mathrm{i}\pi(l-1)\left(\cos\theta_i - \cos\theta_i^*\right)} \frac{\sin\left(\pi l\left(\cos\theta_i - \cos\theta_i^*\right)\right)}{\sin\left(\pi\left(\cos\theta_i - \cos\theta_i^*\right)\right)}. \tag{20}$$

In particular, using (20), after some calculations, the result in (18) can be rewritten as

$$\left|\cos\Omega_i\right| = \left|\frac{\sin\left(\pi l\left(\cos\theta_i - \cos\theta_i^*\right)\right)}{l\sin\left(\pi\left(\cos\theta_i - \cos\theta_i^*\right)\right)}\right|. \tag{21}$$

Specifically, by expressing (20) via the formula of

$$\mathrm{sinc}\left(x\right) = \sin\left(\pi x\right)\frac{1}{\pi x}, \tag{22}$$

one can find that for $l \to \infty$, $f\left(\tau_i\right)$ can be rewritten as [58]

$$\lim_{l\to\infty} f\left(\tau_i\right) = e^{\mathrm{i}\pi l\tau_i}\,\mathrm{sinc}\left(l\tau_i\right). \tag{23}$$

The function $\left|f\left(\tau_i\right)\right|$ for different values of τ_i is depicted in Fig. 1. The function picks up the $\left|f\left(\tau_i\right)\right| = 1$ maximum at $\tau_i = 0$, with a period $r = 1$. For l sub-channels, a period yields l values.

Next, we utilize function $f\left(\cdot\right)$ to derive the $\mathcal{R}_{\phi_i}$ subcarrier domain representation of $\mathcal{N}_i$. Function $f\left(\tau_i\right)$ at a given θ_i formulates a plot

$$\mathrm{p} : \left(\cos\theta_i, \left|f\left(\tau_i\right)\right|\right), \tag{24}$$

where from the $r = 1$ periodicity of $f\left(\cdot\right)$ follows that the main loops are obtained at

$$\cos\theta_i = \cos\theta_i^*. \tag{25}$$

The plot $\left|f\left(\tau_i\right)\right|$ as a function of $\cos\theta_i$ is depicted in Fig. 2, for $\theta_i^* = \pi/2$, $l = 2$.

From the bases $b\left(\cdot\right)$ of (15) and (16), the Fourier bases $b\left(\frac{k}{l}\right)$ and $b\left(\frac{i}{l}\right), i, k = 0, \ldots, l-1$, is defined as follows.

The set S_b of the $\mathcal{R}_\phi$ orthonormal basis over the $\mathcal{C}^l$ complex space of the $\mathcal{R}_\phi$ subcarrier domain representation can be defined as

$$\mathrm{S}_b = \left\{b\left(0\right), b\left(\tfrac{1}{l}\right), \ldots, b\left(\tfrac{l-1}{l}\right)\right\} \in \mathcal{C}^l, \tag{26}$$

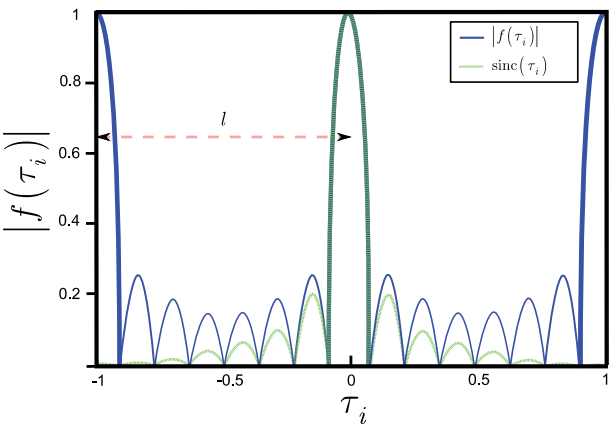

Fig. 1 The function $\left|f\left(\tau_i\right)\right|$ (blue) for different values of τ_i. The period of the function is $r = 1$. The sinc function (green) is approximated with an arbitrary precision in the asymptotic limit of $l \to \infty$

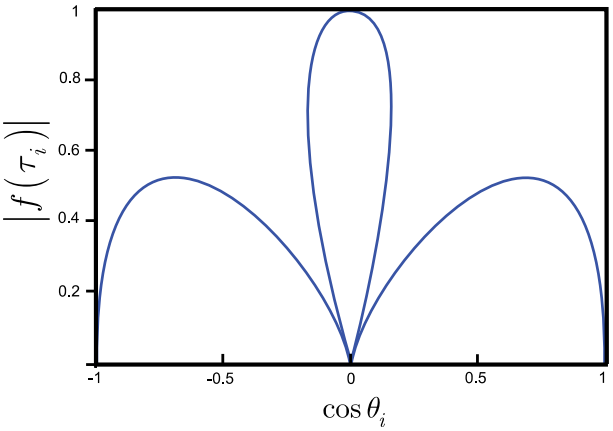

Fig. 2 The $\mathcal{R}_{\phi_i}$ subcarrier domain representation of $\mathcal{N}_i$, at $\theta_i^* = \pi/2$, $l = 2$. The function $|f(\tau_i)|$ picks up the maximum at $\tau_i = 0$

and $b\left(\frac{k}{l}\right)$ is an $l \times 1$ matrix as

$$b(0) = \frac{1}{\sqrt{l}} \begin{pmatrix} 1 \\ 1 \\ 1 \\ \vdots \\ 1 \end{pmatrix}, \tag{27}$$

and

$$b\left(\frac{k}{l}\right) = \frac{1}{\sqrt{l}} \begin{pmatrix} 1 \\ e^{\frac{-i2\pi k}{l}} \\ e^{\frac{-i2\pi 2k}{l}} \\ \vdots \\ e^{\frac{-i2\pi(l-1)k}{l}} \end{pmatrix}, \tag{28}$$

while the $b\left(\frac{i}{l}\right)$ $l \times 1$ matrix is precisely as

$$b\left(\frac{i}{l}\right) = \frac{1}{\sqrt{l}} \begin{pmatrix} 1 \\ e^{\frac{-i2\pi i}{l}} \\ e^{\frac{-i2\pi i2}{l}} \\ \vdots \\ e^{\frac{-i2\pi i(l-1)}{l}} \end{pmatrix}. \tag{29}$$

Precisely, using the orthonormal basis of (26), the result in (20) can be rewritten as

$$f(\tau_i) = b(0)^{\dagger} b(\tau_i). \tag{30}$$

Specifically, the expression of (30) allows us to redefine the plot of (24) to express $b\left(\frac{k}{l}\right)$ as follows:

$$\mathrm{p}_{b\left(\frac{k}{l}\right)}: \left(\cos\theta_i, \left|f\left(\cos\theta_i - \tfrac{k}{l}\right)\right|\right), \tag{31}$$

and thus the maximum values are obtained at

$$\cos\theta_i = \tfrac{k}{l}. \tag{32}$$

Particularly, at a given l, evaluating f at $k = 1, \ldots, l-1$ yields the following values [58]:

$$f\left(\tfrac{k}{l}\right) = 0, \tag{33}$$

and

$$f\left(\tfrac{-k}{l}\right) = f\left(\tfrac{l-k}{l}\right). \tag{34}$$

In particular, the $\mathrm{A}\left(\mathcal{N}_i\right)$ parameter is called the virtual gain of the $\mathcal{N}_i$ sub-channel transmittance coefficient, and without loss of generality, it is defined as

$$\mathrm{A}\left(\mathcal{N}_i\right) = x_i, \tag{35}$$

where x_i is a real variable, $x_i \geq 0$.

From (15), (16), and (35), $\mathbf{T}\left(\mathcal{N}\right)$ can be expressed as

$$\mathbf{T}\left(\mathcal{N}\right) = \sum_{i=0}^{l-1} \mathrm{A}\left(\mathcal{N}_i\right) b\left(\cos\theta_i\right) b\left(\cos\theta_i^*\right)^{\dagger}. \tag{36}$$

By exploiting the properties of the Fourier transform [58–60], for a given $\cos\theta_i^*$ and $\cos\theta_i$, $\mathcal{R}_\phi\left(\mathbf{T}\left(\mathcal{N}\right)\right)$ can be rewritten as

$$\begin{aligned}
\mathcal{R}_\phi\left(\mathbf{T}\left(\mathcal{N}\right)\right) &= \sum_{i=0}^{l-1}\sum_{k=0}^{l-1} b\left(\tfrac{k}{l}\right)^{\dagger} T_i\left(\mathcal{N}_i\right) b\left(\tfrac{i}{l}\right) \\
&= \sum_{i=0}^{l-1}\sum_{k=0}^{l-1} b\left(\tfrac{k}{l}\right)^{\dagger} \mathrm{A}\left(\mathcal{N}_i\right) b\left(\cos\theta_i\right) b\left(\cos\theta_i^*\right)^{\dagger} b\left(\tfrac{i}{l}\right) \\
&= \sum_{i=0}^{l-1}\sum_{k=0}^{l-1} x_i b\left(\tfrac{k}{l}\right)^{\dagger} b\left(\cos\theta_i\right) b\left(\cos\theta_i^*\right)^{\dagger} b\left(\tfrac{i}{l}\right).
\end{aligned} \tag{37}$$

Specifically, in (37), for the representation of term $b\left(\cos\theta_i^*\right)^{\dagger} b\left(i/l\right)$ [58], set $S^{\mathcal{R}_{\phi_i}}$ can be defined for the $\mathcal{R}_{\phi_i}$ domain of $\mathcal{N}_i$ as

$$S^{\mathcal{R}_\phi}: \left|\cos\theta_i - \left(\tfrac{k}{l}\right)\right| < \tfrac{1}{l}. \tag{38}$$

The set $S^{\mathcal{R}_\phi}$ in the subcarrier domain representation for $\theta_i^* = \pi/2$, $l = 2$ and $k = 0, \ldots, l-1$, is illustrated by the dashed area in Fig. 3. The $b\left(0\right), b\left(\frac{1}{l}\right), \ldots, b\left(\frac{l-k}{l}\right)$ basis vectors of $\mathcal{R}_\phi$ for $l = 2$ are also depicted, evaluated via (31).

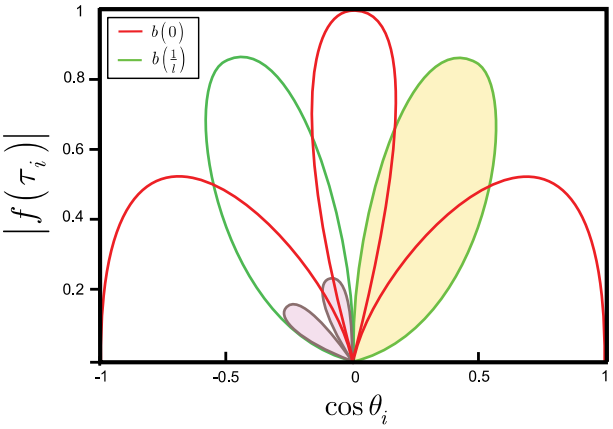

Fig. 3 The set $S^{\mathcal{R}_\phi}$ (dashed areas) for $\theta_i^* = \pi/2$, $l = 2$ Gaussian sub-channels and $k = 0, \ldots l-1$. The curves (red, green) depict the basis vectors $b\,(0)$, $b\left(\frac{1}{l}\right)$ of $\mathcal{R}_\phi$

Putting the pieces together, from (37), $\mathcal{R}_{\phi_i}\left(T_i\left(\mathcal{N}_i\right)\right)$ of a given Gaussian sub-channel $\mathcal{N}_i$ is yielded as

$$\begin{aligned}\mathcal{R}_{\phi_i}\left(T_i\left(\mathcal{N}_i\right)\right) &= \sum_{k=0}^{l-1} b\left(\tfrac{k}{l}\right)^{\dagger} T_i\left(\mathcal{N}_i\right) b\left(\tfrac{i}{l}\right) \\ &= \sum_{k=0}^{l-1} \mathrm{A}\left(\mathcal{N}_i\right) b\left(\tfrac{k}{l}\right)^{\dagger} b\left(\cos\theta_i\right) b\left(\cos\theta_i^*\right)^{\dagger} b\left(\tfrac{i}{l}\right).\end{aligned} \tag{39}$$

□

3.1 Statistics of Subcarrier Domain Sub-channel Transmission

Theorem 2 *(Transmittance of the Gaussian sub-channels). For arbitrary θ_i^*, the magnitude $\left|\mathcal{R}_{\phi_i}\left(T_i\left(\mathcal{N}_i\right)\right)\right|$ of $\mathcal{R}_{\phi_i}\left(T_i\left(\mathcal{N}_i\right)\right)$ of a given $\mathcal{N}_i$ is maximized in the asymptotic limit of $\cos\Omega_i \to 1$, where $\Omega_i = \theta_i - \theta_i^*$. Averaging over the statistics $\mathcal{S}\left(\mathcal{R}_\phi\left(\mathbf{T}\left(\mathcal{N}\right)\right)\right) \in \mathcal{CN}\left(0, \sigma^2_{\mathbf{T}(\mathcal{N})}\right)$, $rank\left(\mathcal{S}\left(\mathcal{R}_\phi\left(\mathbf{T}\left(\mathcal{N}\right)\right)\right)\right) = \min\left(|S_i|, |S_k|\right)$, where the cardinality of sets S_i, S_k identifies the number of non-zero rows and columns of $\mathcal{R}_{\phi_i}\left(\mathbf{T}\left(\mathcal{N}\right)\right)$.*

Proof First, we recall $\mathcal{R}_{\phi_i}\left(T_i\left(\mathcal{N}_i\right)\right)$ from (39) and express $\left|\mathcal{R}_{\phi_i}\left(T_i\left(\mathcal{N}_i\right)\right)\right|$ as

$$\left|\mathcal{R}_{\phi_i}\left(T_i\left(\mathcal{N}_i\right)\right)\right| = \left|\sum_{k=0}^{l-1} x_i b\left(\tfrac{k}{l}\right)^{\dagger} b\left(\cos\theta_i\right) b\left(\cos\theta_i^*\right)^{\dagger} b\left(\tfrac{i}{l}\right)\right|. \tag{40}$$

For a given θ_i^*, the values of angle θ_i has the following statistical impacts on (40).

Without loss of generality, let parameters i and k be fixed as

$$i, k = \{C, C\}, \tag{41}$$

where $C > 0$ is a real variable.

Particularly, for the $\mathcal{N}_i$ sub-channels, the $\left|\mathcal{R}_{\phi_i}\left(T_i\left(\mathcal{N}_i\right)\right)\right|$ magnitudes formulate a set

$$\partial = \left\{\left|\mathcal{R}_{\phi_i}\left(T_i\left(\mathcal{N}_i\right)\right)\right|, i = 0, \ldots, l-1\right\}. \tag{42}$$

Let

$$\Omega_i = \theta_i - \theta_i^*, \tag{43}$$

and let s be the number of sub-channels for which $\left|\mathcal{R}_{\phi_i}\left(T_i\left(\mathcal{N}_i\right)\right)\right| \approx 0$.

Specifically, for ∂, let determine Ω_i the value of k as

$$k = \left\{\begin{array}{l} k \in [0, 2C], \text{ if } |\Omega_i| \to \pi \\ k = i = C, \text{ if } |\Omega_i| = 0 \end{array}\right\}. \tag{44}$$

Let us define a $\mathcal{G}_0$ initial subset with $|\mathcal{G}_0| = s_0$, as

$$\mathcal{G}_0 = \left\{\left|\mathcal{R}_{\phi_j}\left(T_j\left(\mathcal{N}_j\right)\right)\right|, j = 0, \ldots, s_0 - 1\right\} \subseteq \partial, \tag{45}$$

where

$$\left|\mathcal{R}_{\phi_j}\left(T_j\left(\mathcal{N}_j\right)\right)\right| \approx 0. \tag{46}$$

In this setting, as $\cos\Omega_i \to 1$, the cardinality of $\mathcal{G}$ increases,

$$\mathcal{G} : \cos\Omega_i \to 1 : |\mathcal{G}| = s > |\mathcal{G}_0| = s_0, \tag{47}$$

while as $\cos\Omega_i \to -1$, the cardinality of $\mathcal{G}$ decreases, thus

$$\mathcal{G} : \cos\Omega_i \to -1 : |\mathcal{G}| = s < |\mathcal{G}_0| = s_0. \tag{48}$$

In particular, as (48) holds, the range of k expands from C to the full domain of $k = [0, 2C]$, and $\left|\mathcal{R}_{\phi_i}\left(T_i\left(\mathcal{N}_i\right)\right)\right|$ decreases, thus

$$\left|\mathcal{R}_{\phi_i}\left(T_i\left(\mathcal{N}_i\right)\right)\right| \approx a, \tag{49}$$

where a is an average which around the $\left|\mathcal{R}_{\phi_i}\left(T_i\left(\mathcal{N}_i\right)\right)\right|$ coefficients stochastically moves [58–60].

The impact of $\cos\Omega_i \to -1$ on $\left|\mathcal{R}_{\phi_i}\left(T_i\left(\mathcal{N}_i\right)\right)\right|$ is depicted in Fig. 4 for $i, k = \{C, C\}$, $i = C = 0.5l$. The maximum transmittance is normalized to unit for $k = 0.5C$. Statistically, the convergence of $\cos\Omega_i \to -1$ improves the range of k and decreases the sub-channel transmittance (see (44)).

Particularly, the degrees of freedom in $\mathcal{R}_\phi\left(\mathbf{T}\left(\mathcal{N}\right)\right)$ can be evaluated through the rank of $\mathcal{R}_\phi\left(\mathbf{T}\left(\mathcal{N}\right)\right)$.

Let us identify the number of non-zero rows and columns of $\mathcal{R}_{\phi_i}\left(\mathbf{T}\left(\mathcal{N}\right)\right)$ via $|S_i|$ and $|S_k|$, of sets S_i, S_k, respectively. By averaging [58–60] over the statistics of

$$\mathcal{S}\left(\mathcal{R}_\phi\left(\mathbf{T}\left(\mathcal{N}\right)\right)\right) \in \mathcal{CN}\left(0, \sigma^2_{T(\mathcal{N})}\right), \tag{50}$$

thus the rank of $\mathcal{S}\left(\mathcal{R}_\phi\left(\mathbf{T}\left(\mathcal{N}\right)\right)\right)$ without loss of generality is expressed as

$$\begin{aligned} \operatorname{rank}\left(\mathcal{S}\left(\mathcal{R}_\phi\left(\mathbf{T}\left(\mathcal{N}\right)\right)\right)\right) &= \min\left(|S_i|, |S_k|\right) \\ &\approx \min\left(\sum\nolimits_l \cos\theta_i, \sum\nolimits_l \cos\theta_i^*\right), \end{aligned} \tag{51}$$

for an arbitrary distribution, by theory [58].

The rank in (51) basically changes in function of the number l of $\mathcal{N}_i$ Gaussian sub-channels utilized for the multicarrier transmission since the increasing l results in more

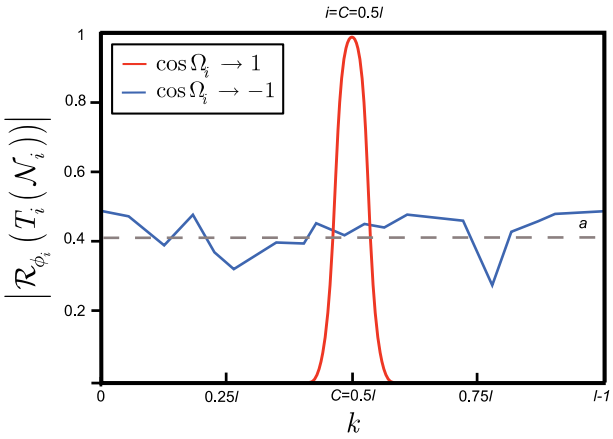

Fig. 4 The impact of $\cos\Omega_i \to -1$ on $\left|\mathcal{R}_{\phi_i}\left(T_i\left(\mathcal{N}_i\right)\right)\right|$ for a fixed $i = C = 0.5l$ on a sub-channel $\mathcal{N}_i$. The parameter range changes to $i, k = \{C, [0, 2C]\}, C = 0.5l$, from $i, k = \{C, C\}$. For $\cos\Omega_i \to 1$, the transmittance picks up the maximum at $k = C = 0.5l$ (red) in a narrow range of $k \approx C$. Statistically, as $\cos\Omega_i \to -1$, the transmittance significantly decreases, moving stochastically around an average a (dashed grey line) within the full range $k = [0, 2C]$

non-zero elements in $\mathcal{S}\left(\mathcal{R}_\phi\left(\mathbf{T}\left(\mathcal{N}\right)\right)\right)$ [58–60]. On the other hand, the rank in (51) also changes in function of θ_i. Specifically, as $\cos\Omega_i \to 1$, the matrix $\mathcal{S}\left(\mathcal{R}_\phi\left(\mathbf{T}\left(\mathcal{N}\right)\right)\right)$ will have significantly decreased number of non-zero entries (see (47)), while for $\cos\Omega_i \to -1$, the rank increases because the number of non-zero entries in (51) increases [58] (see (48)).

These statements can be directly extended to the diversity, since the div $(\cdot)$ diversity function of $\mathcal{S}\left(\mathcal{R}_\phi\left(\mathbf{T}\left(\mathcal{N}\right)\right)\right)$ is evaluated via the number of non-zero entries in $\mathcal{S}\left(\mathcal{R}_\phi\left(\mathbf{T}\left(\mathcal{N}\right)\right)\right)$,

$$\operatorname{div}\left(\mathcal{S}\left(\mathcal{R}_\phi\left(\mathbf{T}\left(\mathcal{N}\right)\right)\right)\right) = \bigcup_{\forall i,k} E_{i,k}\left(\mathcal{S}\left(\mathcal{R}_\phi\left(\mathbf{T}\left(\mathcal{N}\right)\right)\right)\right) \neq 0, \tag{52}$$

where $E_{i,k}$ identifies an (i, k) entry of $\mathcal{S}\left(\mathcal{R}_\phi\left(\mathbf{T}\left(\mathcal{N}\right)\right)\right)$. Precisely, from (52) follows that $\operatorname{div}\left(\mathcal{S}\left(\mathcal{R}_\phi\left(\mathbf{T}\left(\mathcal{N}\right)\right)\right)\right)$ increases with the number l of Gaussian sub-channels. □

4 Subcarrier Domain of Multiuser Multicarrier CVQKD

Lemma 1 *(Subcarrier domain of multiple-access multicarrier CVQKD). The* $\mathcal{R}_\phi\left(\mathbf{T}\left(\mathcal{N}\right)\right)$ *of* $\mathbf{T}\left(\mathcal{N}\right)$ *in a* K_{in}, K_{out} *multiuser setting is* $\mathcal{R}_\phi^{K_{in},K_{out}}\left(\mathbf{T}\left(\mathcal{N}\right)\right) = U_{K_{out}}\mathbf{T}\left(\mathcal{N}\right)U_{K_{out}}$*, where* $U_{K_{out}}$ *is a* $K_{out} \times K_{out}$ *unitary* $U_{K_{out}} = \frac{1}{\sqrt{K_{out}}} e^{\frac{-i2\pi ik}{K_{out}}}$*,* $i, k = 0, \ldots, K_{out} - 1$.

Proof Let K_{in}, K_{out} be the number of transmitter and receiver users in a multiple access multicarrier CVQKD [8], and let $\mathbf{Z}$ be the K_{in} dimensional input of the K_{in} users. The Gaussian CV subcarriers formulate the K_{in} dimensional vector

$$\mathbf{D} = U_{K_{in}}\mathbf{Z}, \tag{53}$$

where $U_{K_{in}}$ stands for the inverse CVQFT unitary operation.

The $U_{K_{in}}$ and $U_{K_{out}}$, $K_{in} \times K_{in}$, $K_{out} \times K_{out}$ unitary matrices at l Gaussian sub-channels are as

$$U_{K_{in}} = \frac{1}{\sqrt{K_{in}}} e^{\frac{\mathrm{i}2\pi ik}{K_{in}}}, i, k = 0, \ldots, K_{in} - 1, \tag{54}$$

and

$$U_{K_{out}} = \frac{1}{\sqrt{K_{out}}} e^{\frac{-\mathrm{i}2\pi ik}{K_{out}}}, i, k = 0, \ldots, K_{out} - 1, \tag{55}$$

which unitary is the CVQFT operation (For further details, see the properties of the multicarrier CVQKD modulation [5,6,8,9].).

Specifically, the output $\mathbf{Y}$ in a K_{in}, K_{out} setting is then yielded as

$$\begin{aligned} \mathbf{Y} &= U_{K_{out}} \mathbf{T}(\mathcal{N}) \left(U_{K_{out}} \mathbf{D}\right) + U_{K_{out}} \Delta \\ &= \left(U_{K_{out}} \mathbf{T}(\mathcal{N}) U_{K_{out}}\right) \mathbf{D} + U_{K_{out}} \Delta \\ &= \mathcal{R}_{\phi}^{K_{in}, K_{out}} (\mathbf{T}(\mathcal{N})) \mathbf{D} + U_{K_{out}} \Delta, \end{aligned} \tag{56}$$

thus without loss of generality

$$\mathcal{R}_{\phi}^{K_{in}, K_{out}} (\mathbf{T}(\mathcal{N})) = U_{K_{out}} \mathbf{T}(\mathcal{N}) U_{K_{out}}. \tag{57}$$

Particularly, by rewriting (37), $\mathcal{R}_{\phi}^{K_{in}, K_{out}} (\mathbf{T}(\mathcal{N}))$ can be expressed as

$$\begin{aligned} &\mathcal{R}_{\phi}^{K_{in}, K_{out}} (\mathbf{T}(\mathcal{N})) \\ &= \sum_{i=0}^{K_{in}-1} \sum_{k=0}^{K_{out}-1} b_{K_{out}} \left(\frac{k}{l}\right)^{\dagger} T_i(\mathcal{N}_i) b_{K_{in}} \left(\frac{i}{l}\right) \\ &= \sum_{i=0}^{K_{in}-1} \sum_{k=0}^{K_{out}-1} b_{K_{out}} \left(\frac{k}{l}\right)^{\dagger} \mathrm{A}(\mathcal{N}_i) b_{K_{out}} (\cos\theta_i) b_{K_{in}} \left(\cos\theta_i^*\right)^{\dagger} b_{K_{in}} \left(\frac{i}{l}\right) \\ &= \sum_{i=0}^{K_{in}-1} \sum_{k=0}^{K_{out}-1} x_i b_{K_{out}} \left(\frac{k}{l}\right)^{\dagger} b_{K_{out}} (\cos\theta_i) b_{K_{in}} \left(\cos\theta_i^*\right)^{\dagger} b_{K_{in}} \left(\frac{i}{l}\right), \end{aligned} \tag{58}$$

where the basis vectors are precisely as

$$b_{K_{out}} (\cos\theta_i) = \frac{1}{\sqrt{K_{out}}} \begin{pmatrix} 1 \\ e^{\frac{-i2\pi l \cos\theta_i}{K_{out}}} \\ e^{\frac{-i2\pi 2l \cos\theta_i}{K_{out}}} \\ \vdots \\ e^{\frac{-i2\pi (K_{out}-1) l \cos\theta_i}{K_{out}}} \end{pmatrix} \tag{59}$$

and

$$b_{K_{in}}\left(\cos\theta_i^*\right)=\frac{1}{\sqrt{K_{in}}}\begin{pmatrix}1\\ e^{\frac{-i2\pi l\cos\theta_i^*}{K_{in}}}\\ e^{\frac{-i2\pi 2l\cos\theta_i^*}{K_{in}}}\\ \vdots\\ e^{\frac{-i2\pi(K_{in}-1)l\cos\theta_i^*}{K_{in}}}\end{pmatrix}, \tag{60}$$

thus

$$b_{K_{out}}\left(\frac{k}{l}\right)=\frac{1}{\sqrt{K_{out}}}\begin{pmatrix}1\\ e^{\frac{-i2\pi k}{K_{out}}}\\ e^{\frac{-i2\pi 2k}{K_{out}}}\\ \vdots\\ e^{\frac{-i2\pi(K_{out}-1)k}{K_{out}}}\end{pmatrix}, \tag{61}$$

and

$$b_{K_{in}}\left(\frac{i}{l}\right)=\frac{1}{\sqrt{K_{in}}}\begin{pmatrix}1\\ e^{\frac{-i2\pi i}{K_{in}}}\\ e^{\frac{-i2\pi i2}{K_{in}}}\\ \vdots\\ e^{\frac{-i2\pi i(K_{in}-1)}{K_{in}}}\end{pmatrix}. \tag{62}$$

Without loss of generality, the function f from (20) can be rewritten as

$$f^{K_{out}}\left(\tau_i\right)=\frac{1}{K_{out}}e^{\frac{\mathrm{i}\pi l(K_{out}-1)\tau_i}{K_{out}}}\frac{\sin(\pi l\tau_i)}{\sin\left(\pi\frac{l}{K_{out}}\tau_i\right)}, \tag{63}$$

with

$$\left|\cos\Omega_i\right|=\left|\frac{\sin\left(\pi l\left(\cos\theta_i-\cos\theta_i^*\right)\right)}{K_{out}\sin\left(\pi\frac{l}{K_{out}}\left(\cos\theta_i-\cos\theta_i^*\right)\right)}\right|, \tag{64}$$

such that

$$f^{K_{out}}\left(\frac{k}{l}\right)=0, \tag{65}$$

and

$$f^{K_{out}}\left(\frac{-k}{l}\right)=f^{K_{out}}\left(\frac{K_{out}-k}{l}\right), k=1,\ldots,K_{out}-1. \tag{66}$$

The maximum values of $f^{K_{out}}\left(\frac{k}{l}\right)$ are obtained at

$$\cos\theta_i=k/l \mod K_{out}/l\ . \tag{67}$$

The subcarrier domain representation $\mathcal{R}_{\phi}^{K_{in},K_{out}}\left(T_i\left(\mathcal{N}_i\right)\right)$ via $\left|f^{K_{out}}\left(\tau_i\right)\right|$ for $K_{out}>l$, at $\theta_i^*=\pi/2$, $l=2$ is shown in Fig. 5.

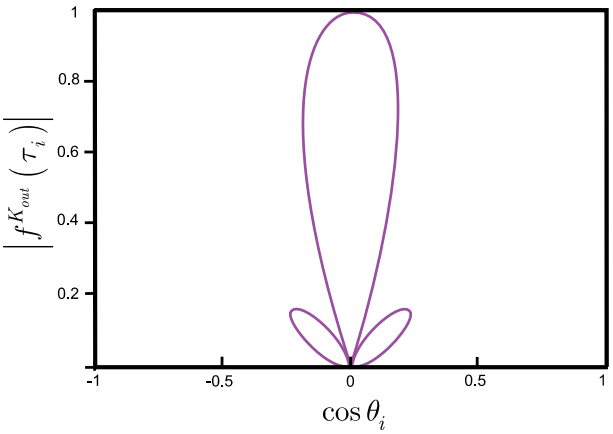

Fig. 5 The function $\left|f^{K_{out}}(\tau_i)\right|$ of $\mathcal{R}_{\phi}^{K_{in},K_{out}}(T_i(\mathcal{N}_i))$ for $K_{out} > l$, at $\theta_i^* = \pi/2$, $l = 2$

The sets $\mathrm{S}_{b_{K_{in}}}$, $\mathrm{S}_{b_{K_{out}}}$ of the $b_{K_{in}}$, $b_{K_{out}}$ orthonormal bases of a K_{in}, K_{out} setting are as

$$\mathrm{S}_{b_{K_{in}}} = \left\{ b_{K_{in}}(0), b_{K_{in}}\left(\tfrac{1}{l}\right), \ldots, b_{K_{in}}\left(\tfrac{K_{in}-1}{l}\right) \right\} \in \mathcal{C}^{K_{in}}, \tag{68}$$

and

$$\mathrm{S}_{b_{K_{out}}} = \left\{ b_{K_{out}}(0), b_{K_{out}}\left(\tfrac{1}{l}\right), \ldots, b_{K_{out}}\left(\tfrac{K_{out}-1}{l}\right) \right\} \in \mathcal{C}^{K_{out}}. \tag{69}$$

□

5 Conclusions

We defined the subcarrier domain for multicarrier CVQKD. In a multicarrier CVQKD protocol, the characterization of the subcarrier domain of a Gaussian sub-channel is provided by the unitary CVQFT transformation, which has a central role in multicarrier CVQKD. The subcarrier domain injects physical attributes to the mathematical model of the Gaussian sub-channels. It provides a natural representation of multicarrier CVQKD and allows us to extend it to a multiple-access multicarrier CVQKD setting. The subcarrier domain representation is a general framework that can be utilized for an arbitrary multicarrier CVQKD scenario. The subcarrier domain also offers an apparatus to formulate the psychical model of the sub-channel transmission, which is particularly convenient for an experimental multicarrier CVQKD scenario.

Acknowledgements Open access funding provided by Budapest University of Technology and Economics (BME). The research reported in this paper has been supported by the National Research, Development and Innovation Fund (TUDFO/51757/2019-ITM, Thematic Excellence Program). This work was partially supported by the National Research Development and Innovation Office of Hungary (Project No. 2017-1.2.1-NKP-2017-00001), by the Hungarian Scientific Research Fund-OTKA K-112125 and in part by the BME Artificial Intelligence FIKP grant of EMMI (BME FIKP-MI/SC).

Author contributions LGY designed the protocol and wrote the manuscript. LGY and SI analyzed the results. All authors reviewed the manuscript.

Funding No relevant funding.

Compliance with Ethical Standards

Conflict of interest We have no competing financial interests.

Research Involving Human Participants This work did not involve any active collection of human data.

Appendix

Multicarrier CVQKD

First we summarize the basic notations of AMQD [5]. The following description assumes a single user, and the use of n Gaussian sub-channels $\mathcal{N}_i$ for the transmission of the subcarriers, from which only l sub-channels will carry valuable information.

In the single-carrier modulation scheme, the j-th input single-carrier state $|\varphi_j\rangle = |x_j + \mathrm{i}p_j\rangle$ is a Gaussian state in the phase space $\mathcal{S}$, with i.i.d. Gaussian random position and momentum quadratures $x_j \in \mathcal{N}\left(0, \sigma^2_{\omega_0}\right)$, $p_j \in \mathcal{N}\left(0, \sigma^2_{\omega_0}\right)$, where $\sigma^2_{\omega_0}$ is the modulation variance of the quadratures. (For simplicity, $\sigma^2_{\omega_0}$ is referred to as the single-carrier modulation variance, throughout.) Particularly, this Gaussian single-carrier is transmitted through a Gaussian quantum channel $\mathcal{N}$. In the multicarrier scenario, the information is carried by Gaussian subcarrier CVs, $|\phi_i\rangle = |x_i + \mathrm{i}p_i\rangle$, $x_i \in \mathcal{N}\left(0, \sigma^2_{\omega}\right)$, $p_i \in \mathcal{N}\left(0, \sigma^2_{\omega}\right)$, where σ^2_{ω} is the modulation variance of the subcarrier quadratures, which are transmitted through a noisy Gaussian sub-channel $\mathcal{N}_i$. Each $\mathcal{N}_i$ Gaussian sub-channel is dedicated for the transmission of one Gaussian subcarrier CV from the n subcarrier CVs. (Note: index i refers to the subcarriers, while index j to the single-carriers throughout the manuscript.) The single-carrier state $|\varphi_j\rangle$ in the phase space $\mathcal{S}$ can be modeled as a zero-mean, circular symmetric complex Gaussian random variable $z_j \in \mathcal{CN}\left(0, \sigma^2_{\omega_{z_j}}\right)$, with variance $\sigma^2_{\omega_{z_j}} = \mathbb{E}\left[|z_j|^2\right]$, and with i.i.d. real and imaginary zero-mean Gaussian random components $\mathrm{Re}\left(z_j\right) \in \mathcal{N}\left(0, \sigma^2_{\omega_0}\right)$, $\mathrm{Im}\left(z_j\right) \in \mathcal{N}\left(0, \sigma^2_{\omega_0}\right)$.

In the multicarrier CVQKD scenario, let n be the number of Alice's input single-carrier Gaussian states. The n input coherent states are modeled by an n-dimensional, zero-mean, circular symmetric complex random Gaussian vector

$$\mathbf{z} = \mathbf{x} + i\mathbf{p} = (z_1, \ldots, z_n)^T \in \mathcal{CN}\left(0, \mathbf{K_z}\right) \tag{A.1}$$

where each z_j can be modeled as a zero-mean, circular symmetric complex Gaussian random variable

$$z_j \in \mathcal{CN}\left(0, \sigma^2_{\omega_{z_j}}\right), z_j = x_j + \mathrm{i}p_j. \tag{A.2}$$

Specifically, the real and imaginary variables (i.e., the position and momentum quadratures) formulate n-dimensional real Gaussian random vectors, $\mathbf{x} = (x_1, \ldots, x_n)^T$ and $\mathbf{p} = (p_1, \ldots, p_n)^T$, with zero-mean Gaussian random variables with densities $f(x_j)$ and

$f(p_j)$ as

$$f\left(x_j\right)=\frac{1}{\sigma_{\omega_0}\sqrt{2\pi}}e^{\frac{-x_j^2}{2\sigma_{\omega_0}^2}},\ f\left(p_j\right)=\frac{1}{\sigma_{\omega_0}\sqrt{2\pi}}e^{\frac{-p_j^2}{2\sigma_{\omega_0}^2}}, \tag{A.3}$$

where $\mathbf{K_z}$ is the $n\times n$ Hermitian covariance matrix of $\mathbf{z}$:

$$\mathbf{K_z}=\mathbb{E}\left[\mathbf{z}\mathbf{z}^{\dagger}\right], \tag{A.4}$$

while $\mathbf{z}^{\dagger}$ is the adjoint of $\mathbf{z}$.

For vector $\mathbf{z}$,

$$\mathbb{E}\left[\mathbf{z}\right]=\mathbb{E}\left[e^{i\gamma}\mathbf{z}\right]=\mathbb{E}e^{i\gamma}\left[\mathbf{z}\right] \tag{A.5}$$

holds, and

$$\mathbb{E}\left[\mathbf{z}\mathbf{z}^{T}\right]=\mathbb{E}\left[e^{i\gamma}\mathbf{z}\left(e^{i\gamma}\mathbf{z}\right)^{T}\right]=\mathbb{E}e^{i2\gamma}\left[\mathbf{z}\mathbf{z}^{T}\right], \tag{A.6}$$

for any $\gamma\in[0,2\pi]$. The density of $\mathbf{z}$ is as follows (if $\mathbf{K_z}$ is invertible):

$$f\left(\mathbf{z}\right)=\frac{1}{\pi^n\det\mathbf{K_z}}e^{-\mathbf{z}^{\dagger}\mathbf{K_z}^{-1}\mathbf{z}}. \tag{A.7}$$

A n-dimensional Gaussian random vector is expressed as $\mathbf{x}=\mathbf{A}\mathbf{s}$, where $\mathbf{A}$ is an (invertible) linear transform from $\mathbb{R}^n$ to $\mathbb{R}^n$, and $\mathbf{s}$ is an n-dimensional standard Gaussian random vector $\mathcal{N}\left(0,1\right)_n$. This vector is characterized by its covariance matrix $\mathbf{K_x}=\mathbb{E}\left[\mathbf{x}\mathbf{x}^T\right]=\mathbf{A}\mathbf{A}^T$, and has density

$$f(\mathbf{x})=\frac{1}{\left(\sqrt{2\pi}\right)^n\sqrt{\det\left(\mathbf{A}\mathbf{A}^T\right)}}e^{-\frac{\mathbf{x}^T\mathbf{x}}{2\left(\mathbf{A}\mathbf{A}^T\right)}}. \tag{A.8}$$

The Fourier transformation $F(\cdot)$ of the n-dimensional Gaussian random vector $\mathbf{v}=(v_1,\ldots,v_n)^T$ results in the n-dimensional Gaussian random vector $\mathbf{m}=(m_1,\ldots,m_n)^T$, as:

$$\mathbf{m}=F\left(\mathbf{v}\right)=e^{\frac{-\mathbf{m}^T\mathbf{A}\mathbf{A}^T\mathbf{m}}{2}}=e^{\frac{-\sigma_{\omega_0}^2\left(m_1^2+\ldots+m_n^2\right)}{2}}. \tag{A.9}$$

In the first step of AMQD, Alice applies the inverse FFT (fast Fourier transform) operation to vector $\mathbf{z}$ (see (A.1)), which results in an n-dimensional zero-mean, circular symmetric complex Gaussian random vector $\mathbf{d}$, $\mathbf{d}\in\mathcal{CN}\left(0,\mathbf{K_d}\right)$, $\mathbf{d}=(d_1,\ldots,d_n)^T$, as

$$\mathbf{d}=F^{-1}\left(\mathbf{z}\right)=e^{\frac{\mathbf{d}^T\mathbf{A}\mathbf{A}^T\mathbf{d}}{2}}=e^{\frac{\sigma_{\omega_0}^2\left(d_1^2+\ldots+d_n^2\right)}{2}}, \tag{A.10}$$

where

$$d_i=x_{d_i}+\mathrm{i}p_{d_i},\ d_i\in\mathcal{CN}\left(0,\sigma_{d_i}^2\right), \tag{A.11}$$

where $\sigma_{\omega_{d_i}}^2=\mathbb{E}\left[\left|d_i\right|^2\right]$ and the position and momentum quadratures of $|\phi_i\rangle$ are i.i.d. Gaussian random variables

$$\mathrm{Re}\left(d_i\right)=x_{d_i}\in\mathcal{N}\left(0,\sigma_{\omega_i}^2\right),\ \mathrm{Im}\left(d_i\right)=p_{d_i}\in\mathcal{N}\left(0,\sigma_{\omega_i}^2\right), \tag{A.12}$$

where $\mathbf{K_d}=\mathbb{E}\left[\mathbf{d}\mathbf{d}^{\dagger}\right]$, $\mathbb{E}\left[\mathbf{d}\right]=\mathbb{E}\left[e^{i\gamma}\mathbf{d}\right]=\mathbb{E}e^{i\gamma}\left[\mathbf{d}\right]$, and $\mathbb{E}\left[\mathbf{d}\mathbf{d}^T\right]=\mathbb{E}\left[e^{i\gamma}\mathbf{d}\left(e^{i\gamma}\mathbf{d}\right)^T\right]=\mathbb{E}e^{i2\gamma}\left[\mathbf{d}\mathbf{d}^T\right]$, for any $\gamma\in[0,2\pi]$.

The $\mathbf{T}(\mathcal{N})$ transmittance vector of $\mathcal{N}$ in the multicarrier transmission is

$$\mathbf{T}(\mathcal{N}) = [T_1(\mathcal{N}_1), \ldots, T_n(\mathcal{N}_n)]^T \in \mathcal{C}^n, \tag{A.13}$$

where

$$T_i(\mathcal{N}_i) = \mathrm{Re}(T_i(\mathcal{N}_i)) + \mathrm{iIm}(T_i(\mathcal{N}_i)) \in \mathcal{C}, \tag{A.14}$$

is a complex variable, which quantifies the position and momentum quadrature transmission (i.e., gain) of the i-th Gaussian sub-channel $\mathcal{N}_i$, in the phase space $\mathcal{S}$, with real and imaginary parts

$$0 \leq \mathrm{Re}T_i(\mathcal{N}_i) \leq 1/\sqrt{2}, \tag{A.15}$$

and

$$0 \leq \mathrm{Im}T_i(\mathcal{N}_i) \leq 1/\sqrt{2}. \tag{A.16}$$

Particularly, the $T_i(\mathcal{N}_i)$ variable has the squared magnitude of

$$|T_i(\mathcal{N}_i)|^2 = \mathrm{Re}T_i(\mathcal{N}_i)^2 + \mathrm{Im}T_i(\mathcal{N}_i)^2 \in \mathbb{R}, \tag{A.17}$$

where

$$\mathrm{Re}T_i(\mathcal{N}_i) = \mathrm{Im}T_i(\mathcal{N}_i). \tag{A.18}$$

The Fourier-transformed transmittance of the i-th sub-channel $\mathcal{N}_i$ (resulted from CVQFT operation at Bob) is denoted by

$$|F(T_i(\mathcal{N}_i))|^2. \tag{A.19}$$

The n-dimensional zero-mean, circular symmetric complex Gaussian noise vector $\Delta \in \mathcal{CN}\left(0, \sigma_\Delta^2\right)_n$ of the quantum channel $\mathcal{N}$, is evaluated as

$$\Delta = (\Delta_1, \ldots, \Delta_n)^T \in \mathcal{CN}(0, \mathbf{K}_\Delta), \tag{A.20}$$

where

$$\mathbf{K}_\Delta = \mathbb{E}\left[\Delta\Delta^\dagger\right]. \tag{A.21}$$

with independent, zero-mean Gaussian random components

$$\Delta_{x_i} \in \mathcal{N}\left(0, \sigma_{\mathcal{N}_i}^2\right), \tag{A.22}$$

and

$$\Delta_{p_i} \in \mathcal{N}\left(0, \sigma_{\mathcal{N}_i}^2\right), \tag{A.23}$$

with variance $\sigma_{\mathcal{N}_i}^2$, for each Δ_i of a Gaussian sub-channel $\mathcal{N}_i$, which identifies the Gaussian noise of the i-th sub-channel $\mathcal{N}_i$ on the quadrature components in the phase space $\mathcal{S}$.

The CVQFT-transformed noise vector can be rewritten as

$$F(\Delta) = (F(\Delta_1), \ldots, F(\Delta_n))^T, \tag{A.24}$$

with independent components $F\left(\Delta_{x_i}\right) \in \mathcal{N}\left(0, \sigma_{F(\mathcal{N}_i)}^2\right)$ and $F\left(\Delta_{p_i}\right) \in \mathcal{N}\left(0, \sigma_{F(\mathcal{N}_i)}^2\right)$ on the quadratures, for each $F(\Delta_i)$. It also defines an n-dimensional zero-mean, circular symmetric complex Gaussian random vector $F(\Delta) \in \mathcal{CN}\left(0, \mathbf{K}_{F(\Delta)}\right)$ with a covariance matrix

$$\mathbf{K}_{F(\Delta)} = \mathbb{E}\left[F(\Delta) F(\Delta)^\dagger\right], \tag{A.25}$$

where $\mathbf{K}_{F(\Delta)} = \mathbf{K}_{\Delta}$, by theory. At a constant subcarrier modulation variance $\sigma^2_{\omega_i}$ for the n Gaussian subcarrier CVs, the corresponding relation is

$$\frac{1}{n}\sum_{i=1}^{n}\sigma^2_{\omega_i} = \sigma^2_{\omega}, \tag{A.26}$$

where $\sigma^2_{\omega_i}$ is the modulation variance of the quadratures of the subcarrier $|\phi_i\rangle$ transmitted by sub-channel $\mathcal{N}_i$. Assuming l good Gaussian sub-channels from the n with constant quadrature modulation variance $\sigma^2_{\omega_i}$, where $\sigma^2_{\omega_i} = 0$ for the i-th unused sub-channel,

$$\sum_{i=1}^{l}\sigma^2_{\omega_i} = l\sigma^2_{\omega} < n\sigma^2_{\omega_0}. \tag{A.27}$$

In particular, from the relation of (A.27), for the transmittance parameters the following relation follows at a given modulation variance $\sigma^2_{\omega_0}$, precisely,

$$\left|T_{AMQD}\left(\mathcal{N}_i\right)\right|^2\sigma^2_{\omega_0} > \left|T\left(\mathcal{N}\right)\right|^2\sigma^2_{\omega_0}, \tag{A.28}$$

where $|T(\mathcal{N})|^2$ is the transmittance of $\mathcal{N}$ in a single-carrier scenario, and

$$\left|T_{AMQD}\left(\mathcal{N}_i\right)\right|^2 = \frac{1}{l}\sum_{i=1}^{l}\left|F\left(T_i\left(\mathcal{N}_i\right)\right)\right|^2. \tag{A.29}$$

For the method of the determination of these l Gaussian sub-channels, see [5]. Alice's i-th Gaussian subcarrier is expressed as

$$|\phi_i\rangle = |d_i\rangle = \left|F^{-1}\left(z\right)\right\rangle. \tag{A.30}$$

A.2 Abbreviations

AMQD	Adaptive Multicarrier Quadrature Division
AWGN	Additive White Gaussian Noise
CV	Continuous-Variable
CVQFT	Continuous-Variable Quantum Fourier Transform
DV	Discrete-Variable
FFT	Fast Fourier Transform
IFFT	Inverse Fast Fourier Transform
MQA	Multiuser Quadrature Allocation
QKD	Quantum Key Distribution
SNR	Signal-to-Noise Ratio
SVD	Singular Value Decomposition

A.3 Notations

The notations of the manuscript are summarized in Table 1.

Table 1 Summary of notations

Notation	*Description*
rank $(\cdot)$	Rank function
div $(\cdot)$	Diversity function
i	Index for the i-th subcarrier Gaussian CV, $\|\phi_i\rangle = x_i + \mathrm{i}p_i$
j	Index for the j-th Gaussian single-carrier CV, $\|\varphi_j\rangle = x_j + \mathrm{i}p_j$
l	Number of Gaussian sub-channels $\mathcal{N}_i$ for the transmission of the Gaussian subcarriers. The overall number of the sub-channels is n. The remaining $n - l$ sub-channels do not transmit valuable information.
x_i, p_i	Position and momentum quadratures of the i-th Gaussian subcarrier, $\|\phi_i\rangle = x_i + \mathrm{i}p_i$
x'_i, p'_i	Noisy position and momentum quadratures of Bob's i-th noisy subcarrier Gaussian CV, $\|\phi'_i\rangle = x'_i + \mathrm{i}p'_i$
x_j, p_j	Position and momentum quadratures of the j-th Gaussian single-carrier $\|\varphi_j\rangle = x_j + \mathrm{i}p_j$
x'_j, p'_j	Noisy position and momentum quadratures of Bob's j-th recovered single-carrier Gaussian CV $\left\|\varphi'_j\right\rangle = x'_j + \mathrm{i}p'_j$
$x_{A,i}$,$p_{A,i}$	Alice's quadratures in the transmission of the i-th subcarrier
$\mathcal{R}_{\phi_i}(T_i(\mathcal{N}_i))$	The subcarrier domain representation of sub-channel $\mathcal{N}_i$, $\mathcal{R}_{\phi_i}(T_i(\mathcal{N}_i)) = UT_i(\mathcal{N}_i)U$, where U is the CVQFT unitary operation
$\|\phi_i\rangle$,$\left\|\phi'_i\right\rangle$	Transmitted and received Gaussian subcarriers. The subcarriers have angles $\theta_i^* \in [0, 2\pi]$, $\theta_i \in [0, 2\pi]$ CVs in the phase space $\mathcal{S}$
$\mathbf{y}^{\mathcal{R}_\phi}$	The subcarrier domain representation of output $\mathbf{y}$, expressed as $\mathbf{y}^{\mathcal{R}_\phi} = \sum_l \mathcal{R}_{\phi_i}(T_i(\mathcal{N}_i))d_i + F(\Delta_i)$
A	The virtual gain of sub-channel $\mathcal{N}_i$, $\mathrm{A}(\mathcal{N}_i) = x_i$, where x_i is a real variable.
$b(\cdot)$	A basis vector of $\mathcal{R}_{\phi_i}$, evaluated as $\mathcal{R}_{\phi_i}(T_i(\mathcal{N}_i)) = \sum_k \mathrm{A}(\mathcal{N}_i)\, b(k/l)^\dagger\, b(\cos\theta_i)\, b\left(\cos\theta_i^*\right)^\dagger b(i/l), k = 0 \ldots l-1$
τ_i	The difference of the cos of phase space angles of the received and transmitted subcarriers, $\tau_i = \cos\theta_i - \cos\theta_i^*$
$\|\cos\Omega_i\|$	The cos of Ω_i, where $\Omega_i = \theta_i - \theta_i^*$ is the angle of the basis vectors $b(\cos\theta_i)$, $b\left(\cos\theta_i^*\right)$. Defined as $\|\cos\Omega_i\| = \left\|b\left(\cos\theta_i^*\right)^\dagger b(\cos\theta_i)\right\|$, $\|\cos\Omega_i\| = \|f(\tau_i)\|$, and $\|\cos\Omega_i\| = \left\|\frac{\sin\left(\pi l\left(\cos\theta_i - \cos\theta_i^*\right)\right)}{l\sin\left(\pi\left(\cos\theta_i - \cos\theta_i^*\right)\right)}\right\|$
$f(\tau_i)$	Defines $\cos\Omega_i$, where Ω_i is the angle of the basis vectors $b(\cos\theta_i)$, $b\left(\cos\theta_i^*\right)$ expressed as $f(\tau_i) = \frac{1}{l}e^{\mathrm{i}\pi(l-1)\left(\cos\theta_i - \cos\theta_i^*\right)}\frac{\sin\left(\pi l\left(\cos\theta_i - \cos\theta_i^*\right)\right)}{\sin\left(\pi\left(\cos\theta_i - \cos\theta_i^*\right)\right)}$
r	The period of function $\|f(\tau_i)\|$
p	The plot of p : $(\cos\theta_i, \|f(\tau_i)\|)$
S_b	The set S_b of the $\mathcal{R}_\phi$ orthonormal basis over the $\mathcal{C}^l$ complex space of the $\mathcal{R}_\phi$ subcarrier domain representation, $\mathrm{S}_b = \left\{b(0), b\left(\frac{1}{l}\right), \ldots, b\left(\frac{l-1}{l}\right)\right\} \in \mathcal{C}^l$
$\mathcal{G}_0$	Set of subcarrier domain representations, $\mathcal{G}_0 = \left\{\left\|\mathcal{R}_{\phi_j}(T_j(\mathcal{N}_j))\right\|, j = 0, \ldots, s_0 - 1\right\} \subseteq \partial$, where $\partial = \left\{\left\|\mathcal{R}_{\phi_i}(T_i(\mathcal{N}_i))\right\|, i = 0, \ldots, l-1\right\}$

Table 1 continued

Notation	*Description*
$E_{i,k}(\mathbf{M})$	The (i,k) entry of matrix $\mathbf{M}$
$U_{K_{out}}$	The unitary CVQFT operation, $U_{K_{out}} = \frac{1}{\sqrt{K_{out}}} e^{\frac{-\mathrm{i}2\pi ik}{K_{out}}}$, $i,k = 0,\ldots,K_{out}-1$, $K_{out} \times K_{out}$ unitary matrix
$U_{K_{in}}$	The unitary inverse CVQFT operation, $U_{K_{in}} = \frac{1}{\sqrt{K_{in}}} e^{\frac{\mathrm{i}2\pi ik}{K_{in}}}$, $i,k = 0,\ldots,K_{in}-1$, $K_{in} \times K_{in}$ unitary matrix
$\mathcal{R}_{\phi}^{K_{in},K_{out}}(\mathbf{T}(\mathcal{N}))$	The subcarrier domain representation of $\mathbf{T}(\mathcal{N})$, expressed as $\mathcal{R}_{\phi}^{K_{in},K_{out}}(\mathbf{T}(\mathcal{N})) = U_{K_{out}}\mathbf{T}(\mathcal{N})U_{K_{out}}$
$b_{K_{out}}(\cdot), b_{K_{in}}(\cdot)$	The basis vectors of the subcarrier domain representation in a K_{in}, K_{out} multiple-access multicarrier CVQKD scenario
$f^{K_{out}}(\tau_i)$	Defines $\cos\Omega_i$, where Ω_i is the angle of the basis vectors $b_{K_{out}}(\cos\theta_i)$, $b_{K_{in}}(\cos\theta_i^*)$ expressed as the angle $f^{K_{out}}(\tau_i) = \frac{1}{K_{out}} e^{\frac{\mathrm{i}\pi l(K_{out}-1)\tau_i}{K_{out}}} \frac{\sin(\pi l\tau_i)}{\sin\left(\pi\frac{l}{K_{out}}\tau_i\right)}$
$\mathrm{S}_{b_{K_{in}}}, \mathrm{S}_{b_{K_{out}}}$	The orthonormal bases of a K_{in}, K_{out} setting, $\mathrm{S}_{b_{K_{in}}} = \left\{b_{K_{in}}(0), b_{K_{in}}\left(\frac{1}{l}\right),\ldots,b_{K_{in}}\left(\frac{K_{in}-1}{l}\right)\right\} \in \mathcal{C}^{K_{in}}$, $\mathrm{S}_{b_{K_{out}}} = \left\{b_{K_{out}}(0), b_{K_{out}}\left(\frac{1}{l}\right),\ldots,b_{K_{out}}\left(\frac{K_{out}-1}{l}\right)\right\} \in \mathcal{C}^{K_{out}}$
$z \in \mathcal{CN}\left(0,\sigma_z^2\right)$	The variable of a single-carrier Gaussian CV state, $\lvert\varphi_i\rangle \in \mathcal{S}$. Zero-mean, circular symmetric complex Gaussian random variable, $\sigma_z^2 = \mathbb{E}\left[\lvert z\rvert^2\right] = 2\sigma_{\omega_0}^2$, with i.i.d. zero mean, Gaussian random quadrature components $x, p \in \mathcal{N}\left(0,\sigma_{\omega_0}^2\right)$, where $\sigma_{\omega_0}^2$ is the variance
$\Delta \in \mathcal{CN}\left(0,\sigma_\Delta^2\right)$	The noise variable of the Gaussian channel $\mathcal{N}$, with i.i.d. zero-mean, Gaussian random noise components on the position and momentum quadratures $\Delta_x, \Delta_p \in \mathcal{N}\left(0,\sigma_{\mathcal{N}}^2\right)$, $\sigma_\Delta^2 = \mathbb{E}\left[\lvert\Delta\rvert^2\right] = 2\sigma_{\mathcal{N}}^2$
$d \in \mathcal{CN}\left(0,\sigma_d^2\right)$	The variable of a Gaussian subcarrier CV state, $\lvert\phi_i\rangle \in \mathcal{S}$. Zero-mean, circular symmetric Gaussian random variable, $\sigma_d^2 = \mathbb{E}\left[\lvert d\rvert^2\right] = 2\sigma_\omega^2$, with i.i.d. zero mean, Gaussian random quadrature components $x_d, p_d \in \mathcal{N}\left(0,\sigma_\omega^2\right)$, where σ_ω^2 is the modulation variance of the Gaussian subcarrier CV state
$F^{-1}(\cdot) = \mathrm{CVQFT}^{\dagger}(\cdot)$	The inverse CVQFT transformation, applied by the encoder, continuous-variable unitary operation
$F(\cdot) = \mathrm{CVQFT}(\cdot)$	The CVQFT transformation, applied by the decoder, continuous-variable unitary operation
$F^{-1}(\cdot) = \mathrm{IFFT}(\cdot)$	Inverse FFT transform, applied by the encoder
$\sigma_{\omega_0}^2$	Single-carrier modulation variance

Table 1 continued

Notation	*Description*
$\sigma_{\omega}^2 = \frac{1}{l}\sum_l \sigma_{\omega_i}^2$	Multicarrier modulation variance. Average modulation variance of the l Gaussian sub-channels $\mathcal{N}_i$
$\|\phi_i\rangle$	The i-th Gaussian subcarrier CV of user U_k, $\|\phi_i\rangle = \left\|\text{IFFT}\left(z_{k,i}\right)\right\rangle = \left\|F^{-1}\left(z_{k,i}\right)\right\rangle = \|d_i\rangle$, where IFFT stands for the Inverse Fast Fourier Transform, $\|\phi_i\rangle \in \mathcal{S}$, $d_i \in \mathcal{CN}\left(0, \sigma_{d_i}^2\right)$, $\sigma_{d_i}^2 = \mathbb{E}\left[\|d_i\|^2\right]$, $d_i = x_{d_i} + \mathrm{i}p_{d_i}$, $x_{d_i} \in \mathcal{N}\left(0, \sigma_{\omega_F}^2\right)$, $p_{d_i} \in \mathcal{N}\left(0, \sigma_{\omega_F}^2\right)$ are i.i.d. zero-mean Gaussian random quadrature components, and $\sigma_{\omega_F}^2$ is the variance of the Fourier transformed Gaussian state
$\left\|\varphi_{k,i}\right\rangle$	The decoded single-carrier CV of user U_k from the subcarrier CV, $\left\|\varphi_{k,i}\right\rangle = \text{CVQFT}\left(\|\phi_i\rangle\right)$, also expressed as $F\left(\|d_i\rangle\right) = \left\|F\left(F^{-1}\left(z_{k,i}\right)\right)\right\rangle = \left\|z_{k,i}\right\rangle$
$\mathcal{N}$	Gaussian quantum channel
$\mathcal{N}_i, i = 1, \ldots, n$	Gaussian sub-channels
$T\left(\mathcal{N}\right)$	Channel transmittance, normalized complex random variable, $T\left(\mathcal{N}\right) = \text{Re}T\left(\mathcal{N}\right) + \mathrm{i}\text{Im}T\left(\mathcal{N}\right) \in \mathcal{C}$. The real part identifies the position quadrature transmission, the imaginary part identifies the transmittance of the position quadrature
$T_i\left(\mathcal{N}_i\right)$	Transmittance coefficient of Gaussian sub-channel $\mathcal{N}_i$, $T_i\left(\mathcal{N}_i\right) = \text{Re}\left(T_i\left(\mathcal{N}_i\right)\right) + \mathrm{i}\text{Im}\left(T_i\left(\mathcal{N}_i\right)\right) \in \mathcal{C}$, quantifies the position and momentum quadrature transmission, with (normalized) real and imaginary parts $0 \leq \text{Re}T_i\left(\mathcal{N}_i\right) \leq 1/\sqrt{2}$, $0 \leq \text{Im}T_i\left(\mathcal{N}_i\right) \leq 1/\sqrt{2}$, where $\text{Re}T_i\left(\mathcal{N}_i\right) = \text{Im}T_i\left(\mathcal{N}_i\right)$.
T_{Eve}	Eve's transmittance, $T_{Eve} = 1 - T\left(\mathcal{N}\right)$
$T_{Eve,i}$	Eve's transmittance for the i-th subcarrier CV
$\mathbf{z}$	A d-dimensional, zero-mean, circular symmetric complex random Gaussian vector that models d Gaussian CV input states, $\mathbf{z} = \mathbf{x} + \mathrm{i}\mathbf{p} = \left(z_1, \ldots, z_d\right)^T$, $\mathcal{CN}\left(0, \mathbf{K_z}\right)$, $\mathbf{K_z} = \mathbb{E}\left[\mathbf{z}\mathbf{z}^{\dagger}\right]$, where $z_i = x_i + \mathrm{i}p_i$, $\mathbf{x} = \left(x_1, \ldots, x_d\right)^T$, $\mathbf{p} = \left(p_1, \ldots, p_d\right)^T$, with $x_i \in \mathcal{N}\left(0, \sigma_{\omega_0}^2\right)$, $p_i \in \mathcal{N}\left(0, \sigma_{\omega_0}^2\right)$ i.i.d. zero-mean Gaussian random variables
$\mathbf{d} = F^{-1}\left(z\right)$	An l-dimensional, zero-mean, circular symmetric complex random Gaussian vector of the l Gaussian subcarrier CVs, $\mathcal{CN}\left(0, \mathbf{K_d}\right)$, $\mathbf{K_d} = \mathbb{E}\left[\mathbf{d}\mathbf{d}^{\dagger}\right]$, $\mathbf{d} = \left(d_1, \ldots, d_l\right)^T$, $d_i = x_i + \mathrm{i}p_i$, $x_i, p_i \in \mathcal{N}\left(0, \sigma_{\omega_F}^2\right)$ are i.i.d. zero-mean Gaussian random variables, $\sigma_{\omega_F}^2 = 1/\sigma_{\omega_0}^2$. The i-th component is $d_i \in \mathcal{CN}\left(0, \sigma_{d_i}^2\right)$, $\sigma_{d_i}^2 = \mathbb{E}\left[\|d_i\|^2\right]$
$\mathbf{y}_k \in \mathcal{CN}\left(0, \mathbb{E}\left[\mathbf{y}_k\mathbf{y}_k^{\dagger}\right]\right)$	A d-dimensional zero-mean, circular symmetric complex Gaussian random vector
$y_{k,m}$	The m-th element of the k-th user's vector $\mathbf{y}_k$, expressed as $\mathbf{y}_{k,m} = \sum_l F\left(T_i\left(\mathcal{N}_i\right)\right)\ F\left(d_i\right) + F\left(\Delta_i\right)$
$F\left(\mathbf{T}\left(\mathcal{N}\right)\right)$	Fourier transform of $\mathbf{T}\left(\mathcal{N}\right) = \left[T_1\left(\mathcal{N}_1\right) \ldots, T_l\left(\mathcal{N}_l\right)\right]^T \in \mathcal{C}^l$, the complex transmittance vector
$F\left(\Delta\right)$	Complex vector, expressed as $F\left(\Delta\right) = e^{\frac{-F(\Delta)^T K_{F(\Delta)} F(\Delta)}{2}}$, with covariance matrix $\mathbf{K}_{F(\Delta)} = \mathbb{E}\left[F\left(\Delta\right)F\left(\Delta\right)^{\dagger}\right]$

Table 1 continued

Notation	*Description*
$\mathbf{y}[j]$	AMQD block, $\mathbf{y}[j] = F(\mathbf{T}(\mathcal{N}))F(\mathbf{d})[j] + F(\Delta)[j]$
$\tau = \|F(\mathbf{d})[j]\|^2$	An exponentially distributed variable, with density $f(\tau) = \left(1/2\sigma_\omega^{2n}\right)e^{-\tau/2\sigma_\omega^2}$, $\mathbb{E}[\tau] \leq n2\sigma_\omega^2$
$T_{Eve,i}$	Eve's transmittance on the Gaussian sub-channel $\mathcal{N}_i$, $T_{Eve,i} = \mathrm{Re}T_{Eve,i} + \mathrm{iIm}T_{Eve,i} \in \mathcal{C}$, $0 \leq \mathrm{Re}T_{Eve,i} \leq 1/\sqrt{2}$, $0 \leq \mathrm{Im}T_{Eve,i} \leq 1/\sqrt{2}$, $0 \leq \left\|T_{Eve,i}\right\|^2 < 1$
d_i	A d_i subcarrier in an AMQD block.
$\nu_{\min}$	The $\min\{\nu_1, \ldots, \nu_l\}$ minimum of the ν_i sub-channel coefficients, where $\nu_i = \sigma_{\mathcal{N}'}^2/\left\|F(T_i(\mathcal{N}_i))\right\|^2$ and $\nu_i < \nu_{Eve}$
σ_ω^2	Modulation variance, $\sigma_\omega^2 = \nu_{Eve} - \nu_{\min}\mathcal{G}(\delta)_{p(x)}$, where $\nu_{Eve} = \frac{1}{\lambda}$, $\lambda = \left\|F\left(T_{\mathcal{N}}^*\right)\right\|^2 = \frac{1}{n}\sum_{i=0}^{n-1}\left\|\sum_{k=0}^{n-1}T_k^* e^{\frac{-i2\pi ik}{n}}\right\|^2$ and $T_{\mathcal{N}}^*$ is the expected transmittance of the Gaussian sub-channels under an optimal Gaussian collective attack
ν_κ	Additional sub-channel coefficient for the correction of modulation imperfections. For an ideal Gaussian modulation, $\nu_\kappa = 0$, while for an arbitrary $p(x)$ distribution $\nu_\kappa = \nu_{\min}\left(1 - \mathcal{G}(\delta)_{p(x)}\right)$, where $\kappa = \frac{1}{\nu_{Eve} - \nu_{\min}\left(\mathcal{G}(\delta)_{p(x)} - 1\right)}$
$\sigma_{\omega_i'}^2$	The constant modulation variance $\sigma_{\omega_i'}^2$ for eigenchannel λ_i, evaluated as $\sigma_{\omega_i'}^2 = \mu - \left(\sigma_{\mathcal{N}'}{}^2/\max_{n_{\min}}\lambda_i^2\right) = \frac{1}{n_{\min}}\sigma_{\omega'}^2$, with a total constraint $\sigma_{\omega'}^2 = \sum_{n_{\min}}\sigma_{\omega_i'}^2 = \frac{1}{l}\sum_l \sigma_{\omega_i}^2 = \sigma_\omega^2$
$\sigma_{\omega''}^2$	The modulation variance of the AMQD multicarrier transmission in the SVD environment. Expressed as $\sigma_{\omega''}^2 = \nu_{Eve} - \left(\sigma_{\mathcal{N}'}^2/\max_{n_{\min}}\lambda_i^2\right)$, where λ_i is the i-th eigenchannel of $F(\mathbf{T})$, $\max_{n_{\min}}\lambda_i^2$ is the largest eigenvalue of $F(\mathbf{T})F(\mathbf{T})^\dagger$, with a total constraint $\frac{1}{l}\sum_l \sigma_{\omega_i''}^2 = \sigma_{\omega''}^2 > \sigma_\omega^2$
$\mathcal{S}(F(\mathbf{T}))$	A statistical model of $F(\mathbf{T})$
$\mathcal{S}\left(\mathcal{R}_{\phi_i}(T_i(\mathcal{N}_i))\right)$	A statistical model of $\mathcal{R}_{\phi_i}(T_i(\mathcal{N}_i))$

References

1. Pirandola, S., Mancini, S., Lloyd, S., Braunstein, S.L.: Continuous-variable quantum cryptography using two-way quantum communication. Nat. Phys. **4**, 726–730 (2008)
2. Grosshans, F., Cerf, N.J., Wenger, J., Tualle-Brouri, R., Grangier, P.: Virtual entanglement and reconciliation protocols for quantum cryptography with continuous variables. Quant. Inf. Comput. **3**, 535–552 (2003)
3. Navascues, M., Acin, A.: Security bounds for continuous variables quantum key distribution. Phys. Rev. Lett. **94**, 020505 (2005)
4. Gyongyosi, L., Imre, S., Nguyen, H.V.: A survey on quantum channel capacities. IEEE Commun. Surv. Tutor. 99, 1 (2018). https://doi.org/10.1109/COMST.2017.2786748

5. Gyongyosi, L., Imre, S.: Adaptive multicarrier quadrature division modulation for long-distance continuous-variable quantum key distribution, Proc. SPIE 9123, Quantum Information and Computation XII, 912307; https://doi.org/10.1117/12.2050095. From Conference Volume 9123, Quantum Information and Computation XII, Baltimore, Maryland, USA (2014)
6. Gyongyosi, L., Imre, S.: Secret key rate proof of multicarrier continuous-variable quantum key distribution. Int. J. Commun. Syst. **32**(4), e3865 (2018). https://doi.org/10.1002/dac.3865
7. Gyongyosi, L., Imre, S.: Diversity Space of Multicarrier Continuous-Variable Quantum Key Distribution. Int. J. Commun. Syst. (2019). https://doi.org/10.1002/dac.4003
8. Gyongyosi, L., Imre, S.: Multiple Access Multicarrier Continuous-Variable Quantum Key Distribution, Chaos, Solitons and Fractals. Elsevier. https://doi.org/10.1016/j.chaos.2018.07.006,ISSN: 0960-0779, (2018)
9. Gyongyosi, L., Imre, S.: Gaussian quadrature inference for multicarrier continuous-variable quantum key distribution. In: Gyongyosi, L., Imre, S. (eds.) Quantum Studies: Mathematics and Foundations. Springer, New York (2019). https://doi.org/10.1007/s40509-019-00183-9
10. Pirandola, S., Garcia-Patron, R., Braunstein, S.L., Lloyd, S.: Direct and reverse secret-key capacities of a quantum channel. Phys. Rev. Lett. **102**, 050503 (2009)
11. Pirandola, S., Serafini, A., Lloyd, S.: Correlation matrices of two-mode Bosonic systems. Phys. Rev. A **79**, 052327 (2009)
12. Pirandola, S., Braunstein, S.L., Lloyd, S.: Characterization of collective Gaussian attacks and security of coherent-state quantum cryptography. Phys. Rev. Lett. **101**, 200504 (2008)
13. Weedbrook, C., Pirandola, S., Lloyd, S., Ralph, T.: Quantum cryptography approaching the classical limit. Phys. Rev. Lett. **105**, 110501 (2010)
14. Weedbrook, C., Pirandola, S., Garcia-Patron, R., Cerf, N.J., Ralph, T., Shapiro, J., Lloyd, S.: Gaussian quantum information. Rev. Mod. Phys. **84**, 621 (2012)
15. Gyongyosi, L., Imre, S.: Geometrical Analysis of Physically Allowed Quantum Cloning Transformations for Quantum Cryptography, Information Sciences, pp. 1–23. Elsevier, Amsterdam (2014). https://doi.org/10.1016/j.ins.2014.07.010
16. Jouguet, P., Kunz-Jacques, S., Leverrier, A., Grangier, P., Diamanti, E.: Experimental demonstration of long-distance continuous-variable quantum key distribution, arXiv:1210.6216v1, (2012)
17. Navascues, M., Grosshans, F., Acin, A.: Optimality of Gaussian attacks in continuous-variable quantum cryptography. Phys. Rev. Lett. **97**, 190502 (2006)
18. Garcia-Patron, R., Cerf, N.J.: Unconditional optimality of Gaussian attacks against continuous-variable quantum key distribution. Phys. Rev. Lett. **97**, 190503 (2006)
19. Grosshans, F.: Collective attacks and unconditional security in continuous variable quantum key distribution. Phys. Rev. Lett. **94**, 020504 (2005)
20. Adcock, M.R.A., Hoyer, P., Sanders, B.C.: Limitations on continuous-variable quantum algorithms with Fourier transforms. New J. Phys. **11**, 103035 (2009)
21. Lloyd, S.: Capacity of the noisy quantum channel. Phys. Rev. A **55**, 1613–1622 (1997)
22. Lloyd, S., Shapiro, J.H., Wong, F.N.C., Kumar, P., Shahriar, S.M., Yuen, H.P.: Infrastructure for the quantum Internet. ACM SIGCOMM Comput. Commun. Rev. **34**, 9–20 (2004)
23. Lloyd, S., Mohseni, M., Rebentrost, P.: Quantum algorithms for supervised and unsupervised machine learning. arXiv:1307.0411 (2013)
24. Lloyd, S., Mohseni, M., Rebentrost, P.: Quantum principal component analysis. Nat. Phys. **10**, 631 (2014)
25. Muralidharan, S., Kim, J., Lutkenhaus, N., Lukin, M.D., Jiang, L.: Ultrafast and fault-tolerant quantum communication across long distances. Phys. Rev. Lett. **112**, 250501 (2014)
26. Kiktenko, E.O., Pozhar, N.O., Anufriev, M.N., Trushechkin, A.S., Yunusov, R.R., Kurochkin, Y.V., Lvovsky, A.I., Fedorov, A.K.: Quantum-secured blockchain. Quantum. Sci. Technol. **3**, 035004 (2018)
27. Gyongyosi, L., Imre, S.: Decentralized base-graph routing for the quantum internet. Phys. Rev. A (2018). https://doi.org/10.1103/PhysRevA.98.022310
28. Van Meter, R.: Quantum Networking. Wiley, ISBN 1118648927, 9781118648926 (2014)
29. Gyongyosi, L., Imre, S.: Singular layer transmission for continuous-variable quantum key distribution, IEEE Photonics Conference (IPC) 2014. IEEE (2014). https://doi.org/10.1109/IPCon.2014.6995246
30. Gyongyosi, L., Imre, S.: Proc. SPIE 9377, Advances in Photonics of Quantum Computing, Memory, and Communication VIII, 937711, https://doi.org/10.1117/12.2076532(2015)
31. Gyongyosi, L., Imre, S.: Gaussian Quadrature Inference for Multicarrier Continuous-Variable Quantum Key Distribution, SPIE Quantum Information and Computation XIV,17–21. Baltimore, Maryland, USA (2016)
32. Imre, S., Balazs, F.: Quantum Computing and Communications—An Engineering Approach, Wiley, ISBN 0-470-86902-X, p. 283 (2005)
33. Petz, D.: Quantum Information Theory and Quantum Statistics, vol. Hiv, p. 6. Springer, Heidelberg (2008)

34. Gyongyosi, L., Imre, S.: Long-distance Continuous-Variable Quantum Key Distribution with Advanced Reconciliation of a Gaussian Modulation. Proceedings of SPIE Photonics West OPTO **2013**, (2013)
35. Pirandola, S.: Capacities of repeater-assisted quantum communications, arXiv:1601.00966 (2016)
36. Pirandola, S.: End-to-end capacities of a quantum communication network. Commun. Phys. **2**, 51 (2019)
37. Gyongyosi, L., Imre, S.: Entanglement-gradient routing for quantum networks. Sci. Rep. Nat. (2017). https://doi.org/10.1038/s41598-017-14394-w
38. Gyongyosi, L., Imre, S.: Entanglement availability differentiation service for the quantum internet. Sci. Rep. Nat. (2018). https://doi.org/10.1038/s41598-018-28801-3
39. Biamonte, J., et al.: Quantum machine learning. Nature **549**, 195–202 (2017)
40. Laudenbach, F., Pacher, C., Fred Fung, C.-H., Poppe, A., Peev, M., Schrenk, B., Hentschel, M., Walther, P., Hubel, H.: Continuous-variable quantum key distribution with Gaussian modulation-The theory of practical implementations. Adv. Quantum Technol. **1800011**, (2018)
41. Shor, P.W.: Scheme for reducing decoherence in quantum computer memory. Phys. Rev. A **52**, R2493–R2496 (1995)
42. Kimble, H.J.: The quantum internet. Nature **453**, 1023–1030 (2008). https://doi.org/10.1038/nature07127
43. Pirandola, S., Laurenza, R., Ottaviani, C., Banchi, L.: Fundamental limits of repeaterless quantum communications. Nat. Commun. **8**, 15043 (2017). https://doi.org/10.1038/ncomms15043
44. Pirandola, S., Braunstein, S.L., Laurenza, R., Ottaviani, C., Cope, T.P.W., Spedalieri, G., Banchi, L.: Theory of channel simulation and bounds for private communication. Quantum Sci. Technol. **3**, 035009 (2018). https://doi.org/10.1088/2058-9565/aac394
45. Laurenza, R., Pirandola, S.: General bounds for sender-receiver capacities in multipoint quantum communications. Phys. Rev. A **96**, 032318 (2017)
46. Bacsardi, L.: On the way to quantum-based satellite communication. IEEE Commun. Mag. **51**(08), 50–55 (2013)
47. Gyongyosi, L., Imre, S.: Low-dimensional reconciliation for continuous-variable quantum key distribution. Appl. Sci. (2018). https://doi.org/10.3390/app8010087,ISSN 2076-3417
48. Shieh, W., Djordjevic, I.: OFDM for Optical Communications. Elsevier, ISBN (eBook): 9780080952062, ISBN (Hardcover): 9780123748799 (2010)
49. Imre, S., Gyongyosi, L.: Advanced Quantum Communications—An Engineering Approach. Wiley-IEEE Press (New Jersey, USA), ISBN-10: 1118002369, ISBN-13: 978-11180023 (2012)
50. Gyongyosi, L., Imre, S.: Proceedings Volume 8997, Advances in Photonics of Quantum Computing, Memory, and Communication VII; 89970C; https://doi.org/10.1117/12.2038532(2014)
51. Gyongyosi, L.: Diversity Extraction for Multicarrier Continuous-Variable Quantum Key Distribution. In Proceedings of the 2016 24th European Signal Processing Conference (EUSIPCO 2016) (2016)
52. Gyongyosi, L., Imre, S.: Eigenchannel decomposition for continuous-variable quantum key distribution. In: Proceedings Volume 9377, Advances in Photonics of Quantum Computing, Memory, and Communication VIII; 937711, https://doi.org/10.1117/12.2076532 (2015)
53. Zhao, W., Liao, Q., Huang, D., et al.: Performance analysis of the satellite-to-ground continuous-variable quantum key distribution with orthogonal frequency division multiplexed modulation. Quant. Inf. Proc. **18**, 39 (2019). https://doi.org/10.1007/s11128-018-2147-8
54. Zhang, H., Mao, Y., Huang, D., Li, J., Zhang, L., Guo, Y.: Security analysis of orthogonal-frequency-division-multiplexing-based continuous-variable quantum key distribution with imperfect modulation. Phys. Rev. A **97**, 052328 (2018)
55. Gyongyosi, L.: Singular value decomposition assisted multicarrier continuous-variable quantum key distribution. Theor. Comput. Sci. (2019). https://doi.org/10.1016/j.tcs.2019.07.029
56. Gyongyosi, L., Imre, S.: Secret key rates of free-space optical continuous-variable quantum key distribution. Int. J. Commun. Syst. (2019). https://doi.org/10.1002/dac.4152
57. Gyongyosi, L., Imre, S.: Statistical quadrature evolution by inference for multicarrier continuous-variable quantum key distribution. In: Quantum Studies: Mathematics and Foundations. Springer, New York (2019). https://doi.org/10.1007/s40509-019-00202-9
58. Tse, D., Viswanath, P.: Fundamentals of Wireless Communication, Cambridge University Press, ISBN-13: 978-0521845274, ISBN-10: 0521845270 (2005)
59. Middlet, D.: An Introduction to Statistical Communication Theory: An IEEE Press Classic Reissue, Hardcover, IEEE, ISBN-10: 0780311787, ISBN-13: 978-0780311787 (1960)
60. Kay, S.: Fundamentals of Statistical Signal Processing, Volumes I–III, Prentice Hall, ISBN-13: 978-0133457117, ISBN-10: 0133457117 (2013)